

Discovery of a Jet-Like Structure at the High Redshift QSO CXOMP J084128.3+131107

D.A. Schwartz, J. Silverman, M. Birkinshaw¹, M. Karovska, T. Aldcroft, W. Barkhouse, P. Green, D.-W. Kim, B. J. Wilkes, D. M. Worrall¹

Harvard-Smithsonian Center for Astrophysics, Cambridge, MA 02138

das@head.cfa.harvard.edu

ABSTRACT

The Chandra Multiwavelength Project (ChaMP) has discovered a jet-like structure associated with a newly recognized QSO at redshift $z=1.866$. The system was $9.4'$ off-axis during an observation of 3C 207. Although significantly distorted by the mirror PSF, we use both a raytrace and a nearby bright point source to show that the X-ray image must arise from some combination of point and extended sources, or else from a minimum of three distinct point sources. We favor the former situation, as three *unrelated* sources would have a small probability of occurring by chance in such a close alignment. We show that interpretation as a jet emitting X-rays via inverse Compton (IC) scattering on the cosmic microwave background (CMB) is plausible. This would be a surprising and unique discovery of a radio-quiet QSO with an X-ray jet, since we have obtained upper limits of $100 \mu\text{Jy}$ on the QSO emission at 8.46 GHz, and limits of $200 \mu\text{Jy}$ for emission from the putative jet.

Subject headings: quasars: general — galaxies: jets — X-rays: galaxies

1. INTRODUCTION

The objectives of the *Chandra* Multiwavelength Project (ChaMP) include identification and categorization of a complete, well-defined sample of serendipitous sources (Kim et al. 2004; Green et al. 2004). The results will be of use, e.g., to study luminosity functions and their evolution, to quantify the newly resolved source(s) of the hard diffuse X-ray background, and to study cosmic structure and clustering of AGN and galaxies. The wide angle nature

¹also, University of Bristol

of this survey also makes it ideal to discover rare and unusual objects suitable for detailed study; e.g., lensed QSOs and X-ray jets.

Schwartz (2002a,b) has pointed out that if the jets observed in X-rays on scales of tens to hundreds of kpc are emitting via IC scattering of the CMB as suggested by Tavecchio et al. (2000) and Celotti et al. (2001), then they will maintain the same apparent surface brightness independent of redshift, and therefore can be detected to arbitrarily large redshifts, up to the epoch at which they form. The *Chandra* observations of such large scale jets in QSOs and powerful FR II radio sources are typically interpreted as IC/CMB emission, (Schwartz et al. 2000; Harris and Krawczynski 2002; Marshall et al. 2001; Sambruna et al. 2001; Siemiginowska et al. 2002). All such interpretations require the assumption that the jet is either relativistically beamed with Doppler factors of order $\delta \sim 3$ to 15, or that the energy density in relativistic electrons grossly exceeds the magnetic field energy density by at least two orders of magnitude. Detection of the X-ray “beacons” predicted by Schwartz (2002a,b) would provide additional evidence that the above assumptions are well founded.

We report the discovery of a candidate for such a system: CXOMP J084128.3+131107, (hereafter called J0841). The X-ray image shows an elongated structure. Despite the broad point response function (PSF) of the *Chandra* telescope at this 9.4’ off-axis angle, we show that at least three point sources would be required to simulate the observed extent. We favor an interpretation of emission from the jet of an optically identified QSO which is close to the peak X-ray intensity. We also mention alternate interpretations. Due to the small probability for three *unrelated* sources to occur by chance in this configuration, such interpretations may be even more unusual.

2. OBSERVATIONS OF J0841

The serendipitous detection of J0841 on the ACIS-I2 chip occurred using the data from obsid 2130, an observation of 3C 207 with ACIS-S3 (Brunetti et al. 2002). Figure 1 shows the X-ray contours superposed on a red-band image. The strongest X-ray peak is coincident within 1.”5 with an $r'=20.9$ mag object. A spectrum of this object (Fig. 2) was obtained in a 10 minute exposure on Magellan using LDSS-2, and clearly shows a broad emission line QSO. The optical data have about 13 Å resolution. The spectrum was cross-correlated against the composite SDSS QSO spectrum (Vanden Berk et al. 2001) to give a redshift 1.866.

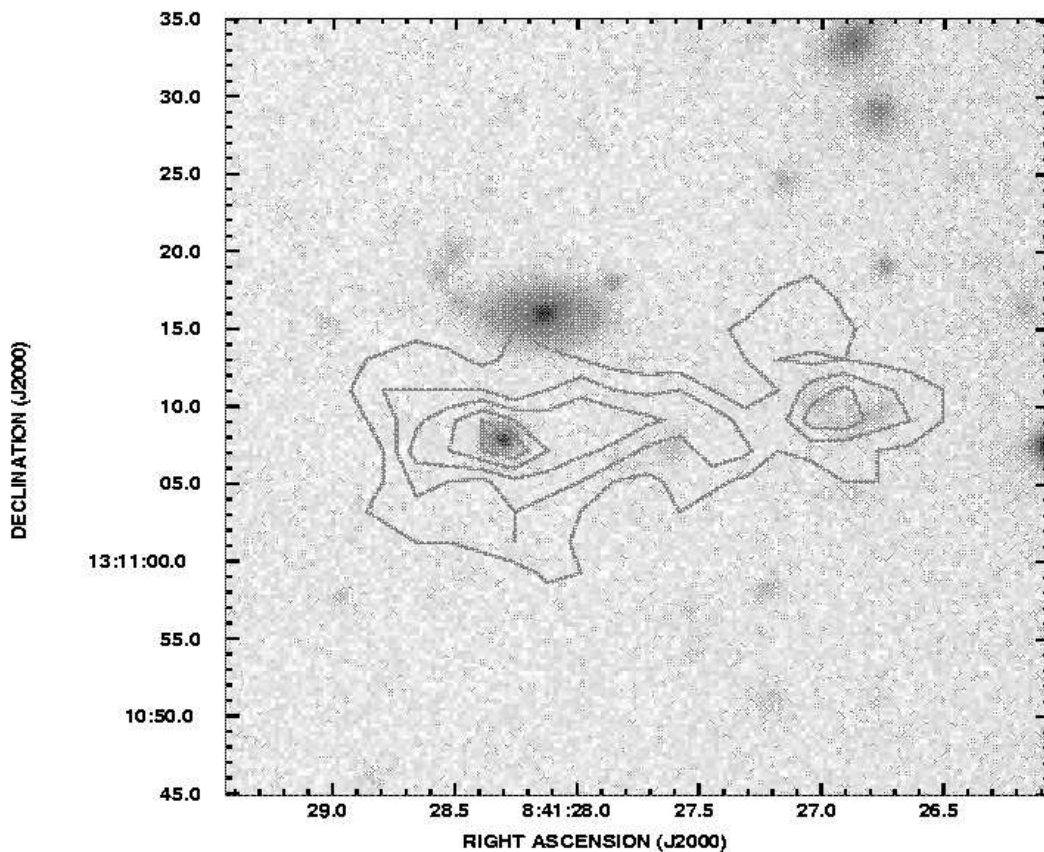


Fig. 1.— X-ray contours (0.5 to 7 keV) in the region of J0841, superposed on a red-band image. Contour levels are 0.25, 0.50, 0.75, 1.0, and 1.25 counts per $0''.98 \times 0''.98$ pixel. Background is 0.03 counts per pixel. The $r'=20.9$ object in the eastern contour peak is a QSO at redshift $z=1.866$. The position difference between the X-ray peak and the optical source is $1''.5$, consistent with the *Chandra* PSF distortion at this large off-axis angle.

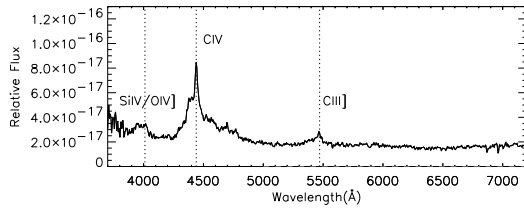


Fig. 2.— Ten minute Magellan exposure of J0841. The broad emission lines give a redshift 1.8661 ± 0.0005

Although the contours in Fig. 1 seem to indicate an extended X-ray structure, one must be careful due to the distorted telescope response at this large off-axis angle. Figure 3 shows the X-ray data in the region of the QSO, together with data around the nearby *Einstein* medium survey point source MS0838.6+1325 (Maccacaro et al. (1991), a $z=0.723$ QSO, also called EMSS 0841+131), which happens to lie in the same *Chandra* field at a similar off-axis angle, 9.3° , and at the nearby azimuth of 247° vs. 265° for J0841. Each is compared with a high fidelity raytrace¹ of a 1.5 keV point source at this off-axis angle and the same azimuth as J0841.² Both QSOs are expected to have relatively hard spectra, for which 1.5 keV is a good mean energy, so we do not expect significant effects due to spectral differences. J0841 is clearly not a single point source.

We now show that two point sources could not produce the observed X-ray structure. Specifically, in the top panel of Fig. 3, taking point sources at the QSO position and at the center of the ellipse marked *B*, we show that region *A* contains a significant excess of counts over background plus those counts which could be attributed to the QSO, plus those counts which could be attributed to the source *B*. The expected counts in box *A* are based on the measured ratio of counts in the ellipse marked *QSO* to the counts in a box marked *A* to the west of the QSO, or a similar box to the east of the QSO (not shown). We derive this predicted ratio both from real data, EMSS 0841+1314, and from a raytrace, and in both cases we predict ≤ 10 counts in box *A*, (including the non-X-ray background). However, we observe 21 counts in box *A*, and the probability of this is less than 0.1

We present the expected number of counts in box *A* in more detail for both methods: based on the raytrace image (middle panel of Fig. 3), and based on the observation of EMSS 0841+131 (bottom panel of Fig. 3). The raytrace contains 1567 counts in the box *A*, and 29945 in the QSO ellipse, for a measured ratio of 0.052. For EMSS 0841+131, after background subtraction, those numbers are 28.3 and 669.6, for a ratio of 0.042 ± 0.008 , consistent with the raytrace prediction. From the observed 78.6 net counts inside the J0841 QSO ellipse (top panel of Fig. 3), after background subtraction, we use the raytrace result of 0.052 to predict 4.1 counts from the quasar would fall in box *A*. We do a similar analysis, but with the raytrace or EMSS 0841+131 source centered in the *B* region. We predict 0.113 and 0.091 ± 0.012 , respectively for the raytrace and for the EMSS 0841+131 data, for the fraction of counts inside the *B* region which would appear in the box *A*. From the net 32.6 counts observed inside region *B*, (top panel of Fig. 3), after background subtraction, the

¹<http://cxc.harvard.edu/chart>

²Note that the *Chandra* point response function is azimuthally asymmetric, see <http://cxc.harvard.edu/ccw.02>

raytrace predicts an additional 3.7 counts in region *A* due to the point source in region *B*. Thus for region *A* in the top panel of Figure 3, we measure 21 counts, and predict 7.8 from the putative point sources *QSO* and *B*, plus 1.7 background counts. The probability of observing 21 or more when 9.5 are expected is 0.086%. We conclude that a minimum of 3 point sources would be needed if J0841 does not have extended X-ray emission.

The ellipses drawn in Fig. 3) are $7'' \times 4''.2$, and are a contour of 62% encircled energy based on EMSS 0841+131, or 55% encircled energy based on the raytrace. The differences in these numbers are consistent with the statistics. For this type of analysis we could have drawn any particular curve around the QSO core – the particular ellipse chosen was convenient but arbitrary. The (unknown) true number of counts is not relevant: we can predict that the contributions to box *A* from a true total point source flux are only about 2.9% and 6.2% from the west and east, respectively.

There are about 100 sources deg^{-2} above a flux of $10^{-14} \text{ ergs cm}^{-2} \text{ s}^{-1}$ (Giacconi et al. 2001). So there is a 2% chance that an unrelated source such as *B* could occur within $30''$ of the QSO. There is then only about a 0.3% chance of an independent third source appearing in a $10'' \times 30''$ region between the first two sources. If we have three point sources, the probability is $\leq 6 \times 10^{-5}$ that they are unrelated. However, the ChaMP survey will eventually find of order 10^3 QSOs brighter than $r'=21$, so there might be as large as 10% probability for one such system of unrelated point sources to be found.

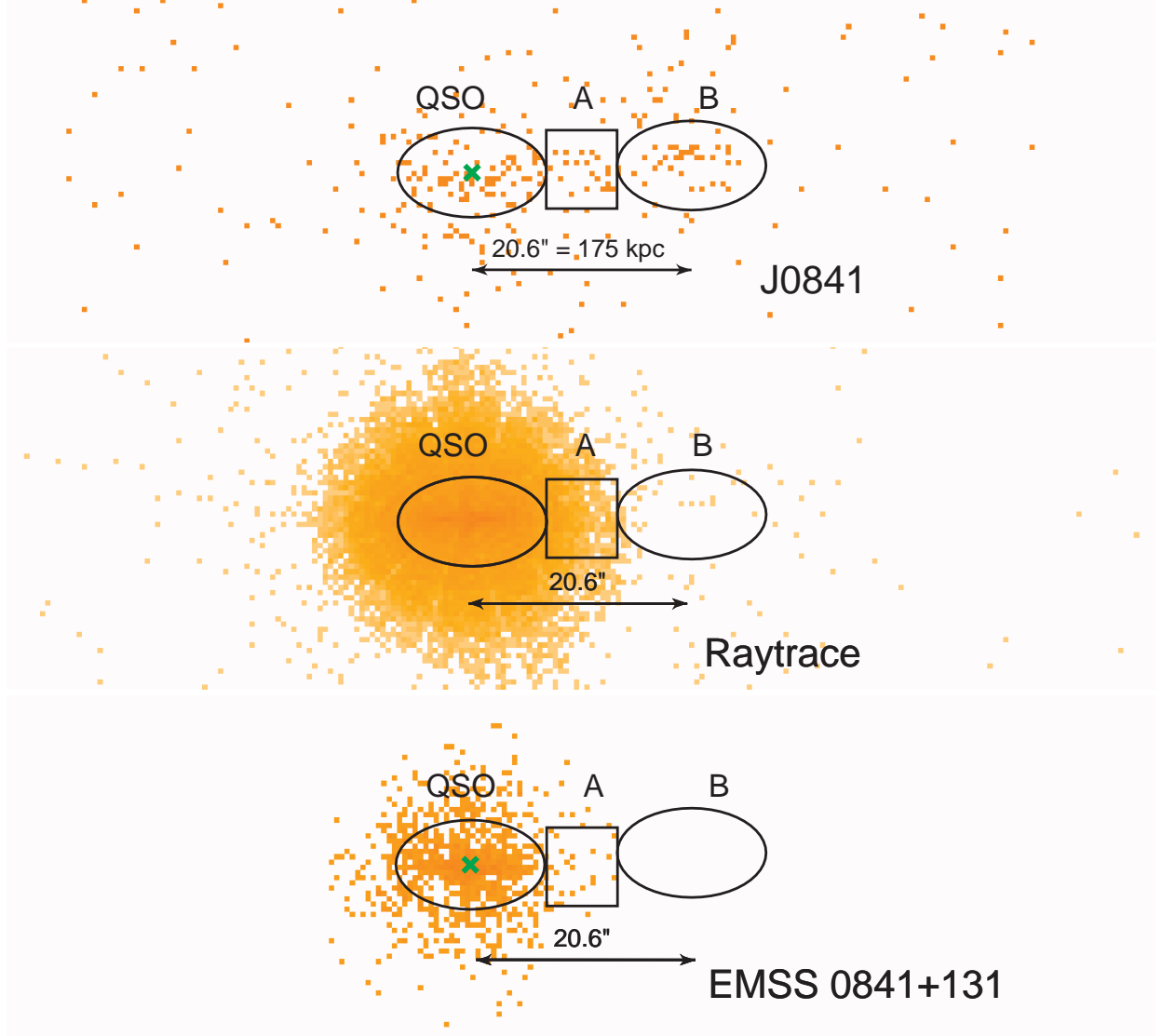


Fig. 3.— X-ray images (0.5 to 7 keV) in $0''.49$ bins. Top to bottom, the J0841 system, a raytrace image of a 1.5 keV point source at the off-axis position of J0841, and a point source, EMSS 0841+1314, from the same observation as J0841. The ellipses labeled *QSO* are centered on the QSO's (green crosses, top and bottom) and the raytrace axis (middle). The ellipse marked *B* is placed on the centroid of counts associated with the concentration $10''$ above the right arrow in the top panel. It is then placed in the same relative position to the raytrace axis and EMSS 0841+1314, in the middle and bottom panels. We show that box *A* in the top panel has excess counts, and therefore represents a third source, based on ratios of the counts inside the *QSO* ellipses to those inside the box *A* in the lower two panels (see text).

3. INTERPRETATION AS AN X-RAY JET

In Figure 3, we will interpret the 78.6 net counts measured in the region indicated *QSO* as from the QSO core, and the 32.6 counts in region *B* and the net 11.5 from region *A* as from the jet. The ellipses shown are 55% encircled energy regions, based on the raytrace result, giving an inferred total counts of 143 from the QSO, and 80 from the jet. This total of 223 inferred counts compares with 275 counts measured in a 25'' radius circle about the QSO, which area contains an expected 73.7 background counts. The observation duration was 37542 seconds, (obsid 2130 of 3C 207). Taking a conversion of 6×10^{-12} ergs $\text{cm}^{-2}\text{s}^{-1}$ per count s^{-1} (appropriate for an X-ray spectral energy index $\alpha=0.7$, and the measured Galactic absorption $n_{\text{H}}=5 \times 10^{20}\text{cm}^{-2}$ (Stark et al. 1992)) gives estimated measured fluxes of 2.3×10^{-14} ergs $\text{cm}^{-2}\text{s}^{-1}$ for the QSO and 1.3×10^{-14} ergs $\text{cm}^{-2}\text{s}^{-1}$ for the jet, in the 0.5 to 7 keV band. At $z=1.866$ this gives luminosities³ of 5.7×10^{44} ergs s^{-1} for the QSO, and 3.2×10^{44} ergs s^{-1} for the jet. The roughly 20'' length of the jet on the sky corresponds to a minimum length of 170 kpc at the redshift $z=1.866$.

Dividing the spectral data into six bins from 1 to 5 keV, and fixing the Galactic absorption, we can estimate an X-ray power-law energy index of 0.3 ± 0.3 for the QSO and 0.5 ± 0.3 for the jet region.

We made a 1 hour VLA observation in the C-array at 8.46 GHz on 10 Jan 2003, and find no emission from the QSO to a 3σ rms noise limit of $100 \mu\text{Jy}^4$, or from the jet to a limit $200 \mu\text{Jy}$. The broad band spectral indexes are $\alpha_{\text{ox}} = 1.43$, and $\alpha_{\text{ro}} < 0.04$, making it radio quiet, with a normal X-ray to optical ratio. Although it would be extremely surprising, and unprecedented, for a radio quiet QSO to have a jet, it can be reasonably interpreted if the jet is highly beamed toward our line of sight, and if the X-rays are being produced by inverse Compton (IC) scattering on the cosmic microwave background (CMB). This is due to the extra factor of $\delta^{1+\alpha}$ (Dermer & Schlickeiser 1994) by which the X-rays are boosted relative to the radio synchrotron emission, where the bulk relativistic Doppler factor δ , is $(\Gamma(1 - \beta \cos \theta))^{-1}$, with Γ being the Lorentz factor of the emitting region which is moving with a velocity βc at an angle θ towards our line of sight. The spectral energy index is α , where flux density $\propto \nu^{-\alpha}$. Tavecchio et al. (2000) and Celotti et al. (2001) showed how this effect could explain the surprisingly large X-ray flux observed from the PKS 0637-752 jet.

³We use $H_0 = 71 \text{ km s}^{-1} \text{ Mpc}^{-1}$ and a flat accelerating universe with $\Omega_0 = 0.27$, and $\Omega_\Lambda = 0.73$.

⁴See <http://www.star.bris.ac.uk/~mb1/j0841.html>

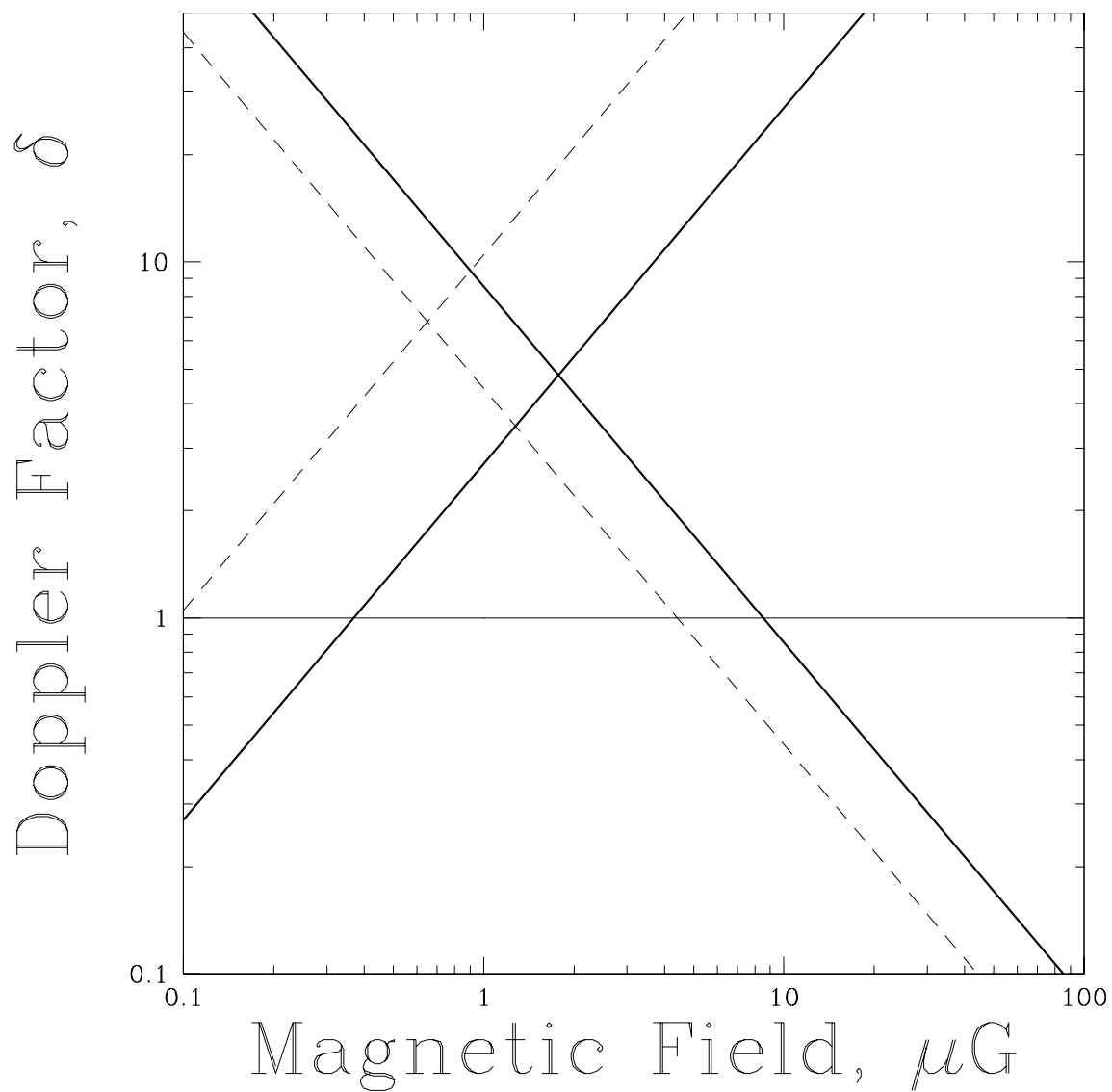


Fig. 4.— Loci of equipartition ($\delta \propto 1/B$) and of X-ray emission via IC/CMB ($\delta \propto B$) in the cases that the 8.46 GHz flux of the jet is at its upper limit of $200 \mu\text{Jy}$ (solid lines), or 10 times weaker (dashed lines). The intersection of solid (or dashed) lines gives a solution for the rest frame magnetic field and the Doppler factor.

Figure 4 applies the analysis of Tavecchio et al. (2000). Here the lines with $\delta \propto 1/B$ show the loci of equipartition between the magnetic fields and particles in the jet rest frame. We assume an electron population, $n(\gamma) \propto \gamma^{-m}$, with spectral index $m=2\alpha+1=2.4$ producing radio emission between 10^6 and 10^{12} Hz, and with an equal energy density in protons. We consider the emitting volume as a cylinder of length $16''.3$. We do not resolve the width of the cylinder, and take the radius to be the $2''.1$ semi-minor axis of the 62% encircled energy ellipse. The lines with $\delta \propto B$ show the loci for which the same electron population giving the radio emission produces the X-rays by IC/CMB. The intersection of the solid lines give a solution for B and δ in the case that the jet flux is at its limit of $200 \mu\text{Jy}$ at 8.46 GHz. In that case, $B = 1.7 \mu\text{G}$ and $\delta = 4.8$. The magnetic field is an upper limit, and the Doppler factor a lower limit, since the radio flux is just an upper limit. The lower limit to δ implies that the jet is within 12° of our line of sight, and therefore at least 670 kpc in length. For comparison, if f_ν were $20 \mu\text{Jy}$, we would have $B=0.65 \mu\text{G}$ and $\delta = 6.8$. Since we do not resolve the jet, it could be very much smaller. This would cause both B and δ to have larger values than numbers quoted. In any case the (B, δ) point must lie to the left and above the upward slanting solid line in Figure 4, and to the right and above a line joining the points where the two solid and two dashed lines intersect.

Electrons with $\gamma = 1000/\Gamma$ produce ≈ 1 keV X-rays when Compton scattering off the microwave background. Such electrons will produce synchrotron radiation at too low a frequency to be observed if $B \lesssim 10 \Gamma^2 \mu\text{G}$. So an alternate explanation for the observed lack of a radio jet is that the electron spectrum breaks, e.g., due to ageing. If the radio break is at 1 GHz and $B=1.7 \mu\text{G}$, the electron spectrum breaks at a Lorentz factor $\leq 10^4$. The lifetime of $\gamma = 10^4$ electrons against Compton scattering on the CMB at $z=1.866$ is about $3.6 \Gamma^{-2} \times 10^6$ years.

4. ALTERNATE INTERPRETATIONS

Some faint galaxies, $r'=23$ to 24 , can be seen more or less overlapping the region of the western X-ray contours in Figure 1. They are much too faint to expect that normal galactic emission provides the X-rays, and the positions cannot be associated with the X-ray emission peaks, especially after adjusting the X-ray contours to coincide with the QSO. Both these objections could be overcome if these objects are a cluster of active galaxies.

Another possibility would be a foreground group of galaxies, at very much lower redshift. This requires only a single unrelated source to be superposed near the QSO by chance. Bauer et al. (2002) reports a density of extended sources at this flux level to be $\approx 10 \text{ deg}^{-2}$, so there would be a 0.2% chance of such a source at this location. Since the ChaMP project

expects to study several thousand sources, such a situation may occur. However, it would be strange that the X-rays do not center on the obvious $z=0.32$ galaxy $8''$ to the north. The X-ray shape is quite distorted, so we would be viewing the cluster in an active and interesting dynamical state. The cluster might be involved in gravitational lensing of the QSO. We might have a failed cluster (Tucker et al. 1995) with only hot gas and no galaxy formation. In case of a foreground cluster, if hot gas overlaps the QSO position future large throughput spectroscopy might use the Krolik and Raymond (1988) test to measure angular diameter distance independently of redshift. Any of these possibilities would result in J0841 being a very exciting system.

5. CONCLUSIONS

Schwartz (2002b) has noted that X-ray emission by IC/CMB should result in X-ray jets being cosmic beacons – maintaining the same surface brightness at any larger redshift. This is because the $(1+z)^{-4}$ cosmic diminution of surface brightness is exactly compensated by the $(1+z)^4$ increase in the energy density of the CMB with redshift. Such an effect does not depend on equipartition, or on relativistic beaming.

The low magnetic field, $\leq 2 \mu\text{G}$, implied by the limits to radio emission is unusual. Fields in clusters of galaxies can approach $1 \mu\text{Gauss}$, while typical jet fields on kpc scales are of order $10 \mu\text{Gauss}$. So the upper limits to magnetic field strengths derived here are somewhat weak for a jet. However, there seems to be no fundamental physics prohibiting massive black holes to produce jets of such low internal energy density. Selection bias against finding radio quiet X-ray jets could explain why such low magnetic field jets have not previously been noticed. Alternately, this object may have a magnetic field much weaker than the equipartition value.

This work was supported in part by NASA contract NAS8-39073 to the *Chandra* X-ray Center, and CXC grants AR2-3009X and GO2-3151C to SAO. We thank D. Harris for discussions and for comments on the manuscript, and D. Jerius for assistance with telescope coordinate systems and the raytrace results. This research used the NASA Astrophysics Data System Bibliographic Services, and the NASA/IPAC Extragalactic Database (NED) which is operated by the Jet Propulsion Laboratory, California Institute of Technology, under contract with the National Aeronautics and Space Administration. We thank the VLA for the allocation of 1 hour of discretionary time. The National Radio Astronomy Observatory is a facility of the National Science Foundation operated under cooperative agreement by Associated Universities, Inc.

REFERENCES

- Bauer, F. E., et al. 2002, *AJ*, 123, 1163
- Brunetti, G., Bondi, M., Comastri, A., & Setti, G. 2002, *A&A*, 381, 795
- Celotti, A., Ghisellini, G., & Chiaberge, M. 2001, *MNRAS*, 321, L1
- Dermer, C. D. & Schlickeiser, R. 1994, *ApJS*, 90, 945
- Giacconi, R. et al. 2001, *ApJ*, 551, 624
- Green, P. J. et al. 2004, *ApJS*, 150, 43
- Harris, D. E., and Krawczynski, H. 2002, *ApJ*, 565, 244
- Kim, D.-W. et al. 2004, *ApJS*, 150, 19
- Krolik, J. H. & Raymond, J. C. 1988, *ApJ*, 335, L39
- Maccacaro, T., della Ceca, R., Gioia, I. M., Morris, S. L., Stocke, J. T. & Wolter, A. 1991, *ApJ*, 374, 117
- Marshall, H. L., et al. 2001, *ApJ*, 549, L167
- Sambruna, R. M., Urry, C. M. Tavecchio, F., Maraschi, L., Scarpa, R., Chartas, G., & Muxlow, T. 2001, *ApJ*, 549, L161
- Siemiginowska, A, Bechtold, J., Aldcroft, T. L., Elvis, M., Harris, D. E., & Dobrzycki, A. 2002, *ApJ*, 570, 543
- Schwartz, D. A., et al. 2000, *ApJ*, 540, L69
- Schwartz, D. A. 2002a, proceedings of “Lighthouses of the Universe,” 538, astro-ph/0110434
- Schwartz, D. A. 2002b, *ApJ*, 569, L75
- Stark A. A., Gammie, C. F., Wilson, R. W., Bally, J., Linke, R. A., Heiles, C., & Hurwitz, M., 1992, *ApJS*, 79, 77
- Tavecchio, F., et al. 2000, *ApJ*, 544, L23
- Tucker, W. H., Tananbaum, H., & Remillard, R. A. 1995, *ApJ*, 444, 532
- Vanden Berk, D. E. 2001, *AJ*, 122, 549